P-ISSN 1859-3585 | E-ISSN 2615-9619

BUCKLING ANALYSIS OF FGM PLATES RESTING ON VARIABLE STIFFNESS ELASTIC FOUNDATIONS

PHÂN TÍCH ỔN ĐỊNH TĨNH CỦA TẤM FGM TỰA TRÊN NỀN ĐÀN HỒI CÓ ĐỘ CỨNG BIẾN ĐỔI

Dao Manh Lan[1], Phan Quang Phuc[2,*], Pham Van Dong[3]

DOI: https://doi.org/10.57001/huih5804.2023.242

ABSTRACT

This paper used the finite element technique to investigate the static buckling behavior of functionally graded material (FGM) plates supported by an elastic base with varying stiffness. The finite element method is formulated using Mindlin's first-order shear deformation theory. FGM plates consist of a combination of ceramic and metal components, with the distribution of these materials following an exponential law. Specifically, the top side of the plate has a higher proportion of ceramic, while the bottom side contains a higher proportion of metal. The dependability of the calculation theory is assessed by a comparison with previously published publications. This article examines the impact of some variables on the static buckling response of FGM plates, including material distribution, elastic foundation parameters, and boundary conditions. The calculation results indicate that the value of the elastic foundation has a significant impact. The critical buckling load and buckling mode shapes of the FGM plate will vary based on the volume distribution of its component materials.

Keywords: *Finite element method, static buckling, Mindlin, plate, elastic foundation.*

TÓM TẮT

Bài báo sử dụng phương pháp phần tử hữu hạn để nghiên cứu ổn định tĩnh của tấm có cơ tính biến đổi (FGM) tựa trên nền đàn hồi có độ cứng biến đổi. Thuật toán phần tử hữu hạn được thiết lập dựa trên lý thuyết biến dạng cắt bậc nhất của Mindlin. Tấm FGM làm từ gốm và kim loại với sự phân bố tỷ lệ thể tích các loại vật liệu tuân theo quy luật hàm số mũ, trong đó mặt trên của tấm giàu gốm và mặt dưới của gốm giàu kim loại. Lý thuyết tính toán được kiểm chứng độ tin cậy bằng việc so sánh với các công trình đã công bố. Trên cơ sở đó, bài báo tiến hành khảo sát ảnh hưởng của một số yếu tố về sự phân bố vật liệu, tham số nền đàn hồi, điều kiện biên đến đáp ứng ổn định của tấm FGM. Các kết quả tính toán cho thấy tùy thuộc vào giá trị của nền đàn hồi, tùy thuộc vào sự phân bố thể tích của các vật liệu thành phần mà đáp ứng tải tới hạn mất ổn định cho tấm cũng như các dạng mất ổn định của tấm FGM cũng sẽ khác nhau.

Từ khóa: *Phương pháp phần tử hữu hạn, ổn định tĩnh, Mindlin, tấm, nền đàn hồi.*

[1]Z131, Vietnam Defence Industry, Vietnam
[2]Z183, Vietnam Defence Industry, Vietnam
[3]Hanoi University of Industry, Vietnam
[*]Email: phucpq@gmail.com
Received: 10/10/2023
Revised: 12/11/2023
Accepted: 16/11/2023

1. INTRODUCTION

The recent development of functionally graded materials (FGM) has garnered significant interest from materials scientists and mechanists worldwide. This is due to its ability to endure substantial loads and exhibit superior resistance to friction and wear compared to conventional materials. Simultaneously, there is no discernible division between the material layers, despite being composed of two distinct materials with disparate mechanical characteristics. FGM functional modification material is required in crucial sectors including construction, particularly in nuclear reactor construction, shipbuilding, and the fabrication of high-temperature-resistant engines. Consequently, several scientists both domestically and internationally have extensively examined the mechanical properties of structures composed of Functionally Graded Materials (FGM), as shown by several notable studies [1-5]. Dat and his research group [1] used the third-order shear deformation theory to determine the precise vibration response of FGM panels with reinforced ribs using the finite element approach. Thom and his colleagues [2] used finite simulation techniques to investigate the thermal stability response of FGM panels using phase-field theory. Vinh and his colleagues used the novel shear deformation theory to determine the inherent vibration frequency of rectangular FGM panels. Quang et al. [4] once again used the precise solution to determine the static bending behavior of shells that had varying mechanical characteristics.

When structures are supported by an additional component, it is feasible to simulate the structure resting on a flexible foundation. However, the uniformity of the foundation's hardness is subject to variation according to certain standards. This scenario may be replicated by modeling a support plate on an elastic basis with varying stiffness characteristics. The calculation and investigation of the mechanical behavior of FGM plate structures on elastic foundations with varying stiffness parameters has significant scientific and practical importance. It has both academic relevance and practical applications in the design and use of FGM structures. Hence, this paper examines the static stability characteristics of panels made of functionally

graded materials (FGM) placed on an elastic basis that has varying stiffness. This work presents significant computer simulations and numerical findings via the use of the finite element approach.

2. PROBLEM MODEL AND SOLUTION SETTING

This article calculates an FGM plate resting on an elastic foundation with variable stiffness as shown in Figure 1. The plate is placed in the Oxyz plane, the geometric parameters of the plate are a, b and h. The stiffness parameter k_w of the elastic foundation varies with x and y coordinates.

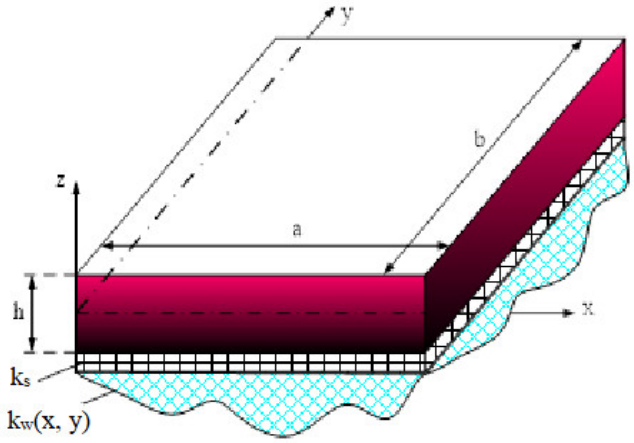

Figure 1. The FGM plate model rests on an elastic foundation with variable stiffness

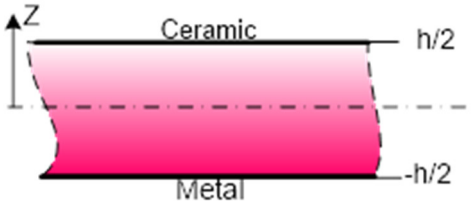

Figure 2. The material is distributed along the thickness of the plate

FGM plates are made of two components: metal and ceramic, with the material volume ratio varying according to the thickness of the panel. The distribution of volume ratio of ceramic (V_c) and volume ratio of metal (V_m) according to the formula.

$$V_m + V_c = 1 \quad (1)$$

where $V_c = \left(\frac{1}{2} + \frac{z}{h}\right)^{n_p}$, n_p is the exponential index of the material volume.

The mechanical properties (Elastic modulus E, Poisson's ratio v) depend on the thickness as follows:

$$\begin{cases} E = E_m + (E_c - E_m)V_c \\ \nu = \nu_m + (\nu_c - \nu_m)V_c \end{cases} \quad (2)$$

Figures 3 and 4 depict the relationship between the volume ratio of ceramic and metal and the material volume exponent, while also considering the variation in plate thickness, *z*. The ratio of ceramic and metal components exhibits a smooth and continuous variation from one side of the plate to the other, with the ceramic-rich plate having a higher ratio on the upper side and the metal-rich plate having a higher ratio on the lower side. Hence, the mechanical characteristics of the material undergo a constant change throughout the FGM plate.

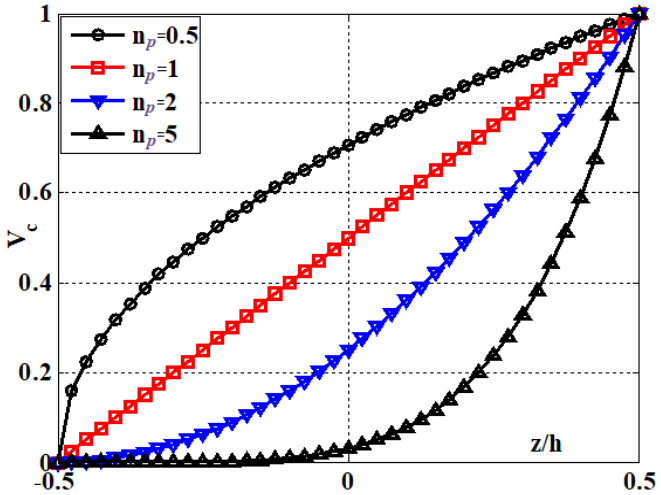

Figure 3. Distribution of V_c (ceramic material ratio) of FGM plates

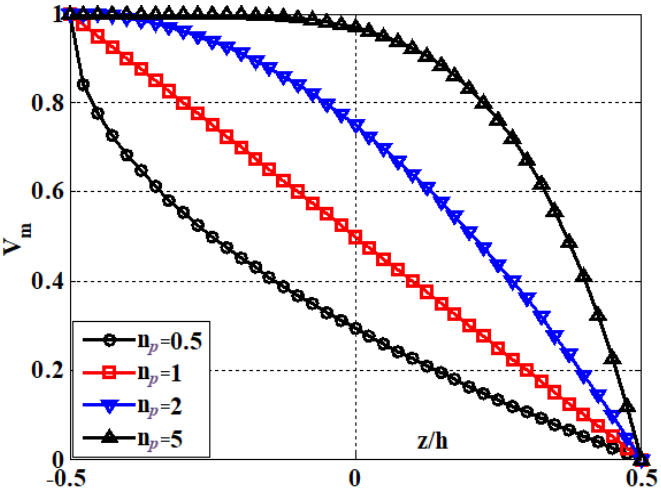

Figure 4. Distribution of metal material ratio V_m of FGM plates

The article uses Mindlin's first-order shear deformation theory, according to which the displacement at any point of the FGM plate has the following expression:

$$\begin{cases} u_x(x,y,z) = u_0 + z\varphi_x \\ v_y(x,y,z) = v_0 + z\varphi_y \\ w_z(x,y,z) = w_z \end{cases} \quad (3)$$

where u_0, v_0, and w are the linear displacements on the neutral surface of the plate according to the coordinate axes Ox, Oy and Oz. φ_x and φ_y are the rotation angles of the cross-section of the plate.

Differentiating the displacement components, we obtain the deformation components of the plate as follows:

$$\begin{cases} \boldsymbol{\beta} = \boldsymbol{\beta}_0 + z\boldsymbol{\beta}_z \\ \boldsymbol{\psi}_s = \boldsymbol{\psi}_{s0} \end{cases} \quad (4)$$

where

$$\boldsymbol{\beta}_0 = \left\{\beta_{0x}, \beta_{0y}, \beta_{0xy}\right\}^T; \boldsymbol{\beta}_z = \left\{\beta_{zx}, \beta_{zy}, \beta_{zxy}\right\}^T;$$
$$\boldsymbol{\psi}_{s0} = \left\{\psi_{xz}, \psi_{yz}\right\}^T; \beta_{0x} = \frac{\partial u_0}{\partial x};$$
$$\beta_{0y} = \frac{\partial v_0}{\partial y}; \beta_{0xy} = \frac{\partial v_0}{\partial x} + \frac{\partial u_0}{\partial y};$$
$$\beta_{zx} = \frac{\partial \varphi_x}{\partial x}; \beta_{zy} = \frac{\partial \varphi_y}{\partial y}; \quad (5)$$
$$\beta_{zxy} = \frac{\partial \varphi_y}{\partial x} + \frac{\partial \varphi_x}{\partial y}; \psi_{xz} = \frac{\partial w}{\partial x} + \varphi_x;$$
$$\psi_{yz} = \frac{\partial w}{\partial y} + \varphi_y;$$

The relationship between stress and strain is as follows:

$$\begin{cases} \begin{Bmatrix} \sigma_x \\ \sigma_y \\ \tau_{xy} \end{Bmatrix} = \frac{E}{1-\nu^2} \begin{bmatrix} 1 & \nu & 0 \\ \nu & 1 & 0 \\ 0 & 0 & \frac{(1-\nu)}{2} \end{bmatrix} \begin{Bmatrix} \beta_x \\ \beta_y \\ \beta_{xy} \end{Bmatrix} = \mathbf{D}_b \boldsymbol{\beta} \\ \begin{Bmatrix} \tau_{xz} \\ \tau_{yz} \end{Bmatrix} = \frac{E_i}{2(1+\nu)} \begin{bmatrix} 1 & 0 \\ 0 & 1 \end{bmatrix} \begin{Bmatrix} \psi_{xz} \\ \psi_{yz} \end{Bmatrix} = \mathbf{D}_s \boldsymbol{\psi} \end{cases} \quad (6)$$

After integrating over the plate thickness, we obtain the normal force, moment and shear force components of the plate as follows:

$$\begin{cases} \begin{Bmatrix} N_x \\ N_y \\ N_{xy} \end{Bmatrix} = \int_{-h/2}^{h/2} \mathbf{D}_b \begin{Bmatrix} \beta_x \\ \beta_y \\ \beta_{xy} \end{Bmatrix} dz = \mathbf{A}_0 \boldsymbol{\beta}_0 + \mathbf{B}_z \boldsymbol{\beta}_z \\ \begin{Bmatrix} M_x \\ M_y \\ M_{xy} \end{Bmatrix} = \int_{-h/2}^{h/2} \mathbf{D}_b \begin{Bmatrix} \beta_x \\ \beta_y \\ \beta_{xy} \end{Bmatrix} z dz = \mathbf{B}_z \boldsymbol{\beta}_0 + \mathbf{D}_z \boldsymbol{\beta}_z \\ \begin{Bmatrix} Q_{xz} \\ Q_{yz} \end{Bmatrix} = \frac{5}{6} \int_{-h/2}^{h/2} \mathbf{D}_s \begin{Bmatrix} \psi_{xz} \\ \psi_{yz} \end{Bmatrix} dz = \mathbf{A}_s \boldsymbol{\psi}_{s0} \end{cases} \quad (7)$$

where the coefficient matrices are determined as follows:

$$\begin{cases} \left\{\mathbf{A}_0, \mathbf{B}_z, \mathbf{D}_z\right\} = \int_{-h/2}^{h/2} \mathbf{D}_b \begin{Bmatrix} \beta_x \\ \beta_y \\ \beta_{xy} \end{Bmatrix} \left\{1, z, z^2\right\} dz \\ \mathbf{A}_s = \frac{5}{6} \int_{-h/2}^{h/2} \mathbf{D}_s \begin{Bmatrix} \psi_{xz} \\ \psi_{yz} \end{Bmatrix} dz \end{cases} \quad (8)$$

Divide the plate into finite elements, each element is triangular, then the displacement at any point of the element will be interpolated through nodal displacement and functions as follows:

$$\left\{u_0, v_0, w, \varphi_x, \varphi_y\right\} = \sum_{i=1}^{3} N_i \left\{u_{0i}, v_{0i}, w_i, \varphi_{xi}, \varphi_{yi}\right\} = \mathbf{N}\mathbf{q}_e \quad (9)$$

where N_i are shape functions, $\mathbf{q}_e$ is the element node displacement vector (including 15 components).

Thus, the strain energy of the plate element has the following form:

$$U_e = \frac{1}{2} \int_{V_e} \left(\boldsymbol{\beta}^T \boldsymbol{\sigma} + \boldsymbol{\psi}^T \boldsymbol{\tau}\right) dV \quad (10)$$

By evaluating the strain and stress components using the shape function and element node displacement vector, we can get the finite formula for the strain energy of the plate element as follows:

$$\begin{aligned} U_e &= \frac{1}{2} \mathbf{q}_e^T \left\{ \int_{S_e} \left(\begin{matrix} \mathbf{B}_1^T \mathbf{A}_0 \mathbf{B}_1 + \mathbf{B}_1^T \mathbf{B}_z \mathbf{B}_2 + \mathbf{B}_2^T \mathbf{B}_z \mathbf{B}_1 \\ + \mathbf{B}_2^T \mathbf{D}_z \mathbf{B}_2 + \mathbf{B}_s^T \mathbf{A}_s \mathbf{B}_s \end{matrix} \right) dS \right\} \mathbf{q}_e \\ &= \frac{1}{2} \mathbf{q}_e^T \mathbf{K}_e \mathbf{q}_e \end{aligned} \quad (11)$$

where $\mathbf{B}_1$, $\mathbf{B}_2$, $\mathbf{B}_s$ are functional differential matrices.

The energy exerted by the elastic foundation on the plate element has the following form:

$$\begin{aligned} U_f &= \frac{1}{2} \int_{S_e} \left(\begin{matrix} k_w \left(1 - c_w \sin\left(\frac{x}{a}\right)\right)\left(1 - c_w \sin\left(\frac{y}{b}\right)\right) w^2 \\ + k_s \left(\left(\frac{\partial w}{\partial x}\right)^2 + \left(\frac{\partial w}{\partial y}\right)^2 \right) \end{matrix} \right) dS \\ &= \frac{1}{2} \mathbf{q}_e^T \mathbf{K}_{fe} \mathbf{q}_e \end{aligned} \quad (12)$$

where k_w and k_s are two coefficients of the elastic foundation as shown in Figure 1, c_w is a parameter showing the change of stiffness according to x and y coordinates.

The energy due to external compressive force acting on the plate element has the following form:

$$U_n = \frac{1}{2} \int_{S_e} \left(P_n \frac{\partial^2 w}{\partial x^2} \right) dS = \frac{1}{2} \mathbf{q}_e^T \mathbf{K}_{Ge} \mathbf{q}_e \quad (13)$$

To establish the balance equation for the plate, the article uses the possible work principle as follows:

$$\begin{aligned} &\delta U_n - \delta U_f - \delta U_e = 0 \\ &\Leftrightarrow \left\{ \sum_e \left(\mathbf{K}_e + \mathbf{K}_f\right) - P_n \sum_e \mathbf{K}_{Ge} \right\} \mathbf{q} = 0 \end{aligned} \quad (14)$$

Solving equation (14) obtains the critical buckling load P_n and the corresponding buckling mode shapes.

3. NUMERICAL RESULTS AND DISCUSSIONS

3.1. Example of accuracy verification

The FGM plate is subjected to compression along two opposing sides. The plate is composed of Al_2O_3 (ceramic) and Al (metal). The width of the plate is denoted as a and the length as b, with a being equal to b. The thickness of the plate, denoted as h, is equal to one twentieth of a. The ceramics have an elastic modulus of 380GPa and a Poisson's ratio of 0.3, whereas the metals have an elastic modulus of 70GPa. The plate is positioned on a two-coefficient elastic basis characterized by parameters $\tilde{k}_1 = k_w \frac{a^4}{D}$, $\tilde{k}_2 = k_s \frac{a^2}{D}$, where $D = \frac{E_m h^3}{12(1-\nu_m^2)}$. The comparison parameter represents

the crucial buckling load of the FGM plate, which is determined using the formula $k_N = P_n a^2/E_m h^3$. Table 1 presents a comparison between the critical buckling load determined using the theoretical approach outlined in the article and the findings reported in literature [6]. The calculations were performed for various elastic foundation values, and the obtained data show a high degree of similarity. These findings exhibit minimal variances, so confirming the dependability of the calculation theory.

Table 1. Comparison results of the critical buckling load k_N of FGM plates resting on an elastic foundation, a/h=20

$(\tilde{k}_1,\tilde{k}_2)$		k = 0	k = 0.5	k = 1	k = 2
$(10^2,10)$	[6]	22.112	15.326	12.426	10.296
	This work	22.368	15.318	12.441	10.333
$(10^3,10^2)$	[6]	43.387	33.049	28.610	25.325
	This work	44.367	33.365	28.875	25.584

3.2. Parameter study

Based on the calculation theory presented above, this section presents the results of numerical calculations to clarify the influence of several material and geometric factors on the static stability response of FGM panels resting on an elastic foundation with variable stiffness. FGM panels have a square shape with the length and width of panels a and b respectively, and panel thickness h. The material's mechanical properties are E_c = 151GPa, E_m= 70GPa, $\nu_c = \nu_m$ = 0.3. If the plate edge has a single support connection, the symbol is S, if the plate edge has a clamp connection, the symbol is C. If the plate edge is free, the symbol is F.

The critical buckling load of the plate is calculated according to the dimensionless formula as follows $N_{cb}=12P_n a^2\left(1-\nu_m^2\right)/E_m\bar{h}^3$, where $\bar{h}$ = a/10. Two dimensionless parameters of the elastic foundation $\hat{k}_w = k_w\frac{a^4}{D_w}$, $\hat{k}_s = k_s\frac{a^2}{D_w}$, với $D_w = \frac{E_m\bar{h}^3}{12\left(1-\nu_m^2\right)}$.

- Effect of elastic foundation stiffness: consider the case of elastic foundation with parameter c_w = 0.5, changing the stiffness of the elastic foundation. The results of calculating the critical buckling load of FGM panels are shown in Tables 2, 3, one can see comments as follows: When increasing the stiffness of the elastic foundation, the plate becomes stiffer, so the ultimate load also increases, meaning the plate is better able to withstand compression. At the same time, when increasing the value of n_p, the proportion of metal components in the plate increases, the plate becomes softer. Therefore, the critical buckling load of the plate is reduced.

Table 2. Critical buckling load N_{cb} of the SSSS FGM plate depend on $\left[\hat{k}_w,\hat{k}_s\right]$, compression along the Ox axis, a/h=20

$\left[\hat{k}_w,\hat{k}_s\right]$	$n_p = 0$	$n_p = 1$	$n_p = 1.5$	$n_p = 2$	$n_p = 10$
[0,0]	8.473	5.903	5.585	5.412	4.691
[10,0]	8.533	5.963	5.645	5.472	4.751
[10,2]	8.937	6.366	6.049	5.875	5.155
[50,5]	9.781	7.210	6.893	6.720	5.999
$[10^2,10]$	11.089	8.518	8.200	8.027	7.306
$[10^3,10^2]$	26.921	23.017	22.529	22.262	21.152

Table 3. Critical buckling load N_{cb} of the SSSS FGM plate depend on $\left[\hat{k}_w,\hat{k}_s\right]$, four edges are subjected to compression, a/h=20

$\left[\hat{k}_w,\hat{k}_s\right]$	$n_p = 0$	$n_p = 1$	$n_p = 1.5$	$n_p = 2$	$n_p = 10$
[0,0]	4.236	2.951	2.792	2.706	2.345
[10,0]	4.266	2.981	2.822	2.736	2.375
[10,2]	4.468	3.183	3.024	2.937	2.577
[50,5]	4.890	3.605	3.446	3.360	2.999
$[10^2,10]$	5.544	4.259	4.100	4.013	3.653
$[10^3,10^2]$	17.296	15.998	15.836	15.748	15.376

- Influence of boundary conditions: This computation is applicable to six distinct boundary condition scenarios. The critical buckling loads for each scenario are shown in Tables 4, 5. These findings demonstrate that altering the boundary conditions directly impacts the critical load of the FGM plate. This is due to the influence of the boundary conditions on the structural stiffness. The plate subjected to CFFF boundary condition exhibits the lowest critical buckling stress, whereas the plate subjected to CCCC boundary condition demonstrates the greatest critical buckling load.

Table 4. Critical buckling load N_{cb} of the SSSS FGM plate depend on boundary conditions, compression along the Ox axis, $\left[\hat{k}_w,\hat{k}_s\right]$ = [100,10], a/h=20

Bc	$n_p = 0$	$n_p = 1$	$n_p = 1.5$	$n_p = 2$	$n_p = 10$
SSSS	11.089	8.518	8.200	8.027	7.306
SCSC	17.041	12.325	11.732	11.405	10.050
SFSF	3.655	3.037	2.961	2.920	2.747
CFFF	2.276	2.062	2.032	2.016	1.945
CFCF	8.557	6.366	6.089	5.935	5.301
CCCC	22.513	16.337	15.557	15.126	13.342

Table 5. Critical buckling load N_{cb} of the SSSS FGM plate depend on boundary conditions, four edges are subjected to compression, $\left[\hat{k}_w,\hat{k}_s\right]$ = [100,10], a/h =20

Bc	$n_p = 0$	$n_p = 1$	$n_p = 1.5$	$n_p = 2$	$n_p = 10$
SSSS	5.544	4.259	4.100	4.013	3.653
SCSC	9.197	6.796	6.496	6.332	5.650
SFSF	3.545	2.908	2.825	2.779	2.725
CFFF	2.220	1.978	1.946	1.927	1.849
CFCF	6.735	5.059	4.848	4.732	4.251
CCCC	12.093	8.806	8.395	8.169	7.231

The first four buckling mode forms of the FGM plate with two boundary conditions and parameters c_w = 0 and c_w = 0.5

P-ISSN 1859-3585 | E-ISSN 2615-9619

are shown in Figures 5 - 8. These forms illustrate that boundary circumstances also impact the buckling modes of the plate. Furthermore, the buckling mode forms are also influenced by the variation in the value of the foundation c_w parameter.

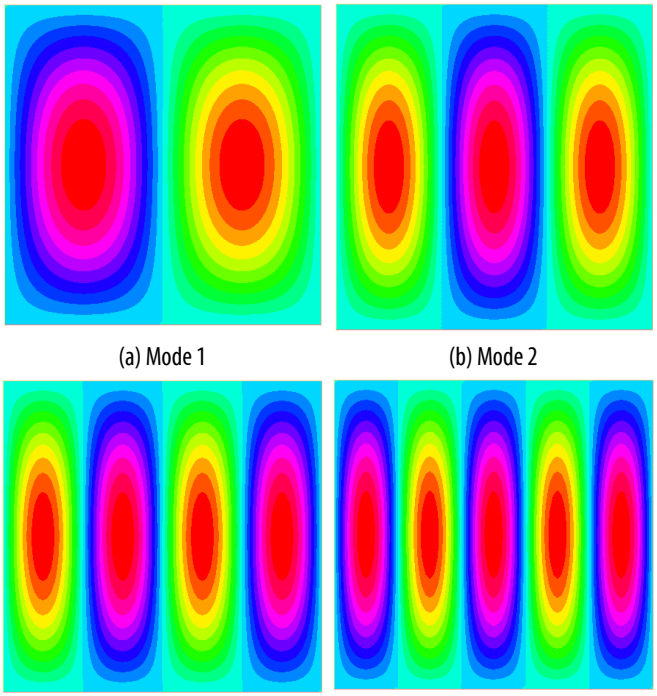

(a) Mode 1 (b) Mode 2

(c) Mode 3 (d) Mode 4

Figure 5. The first four buckling mode shapes of the FGM plate corresponding to the SSSS case, $\left[\hat{k}_w, \hat{k}_s\right] = [10^4, 100]$, $c_w = 0$

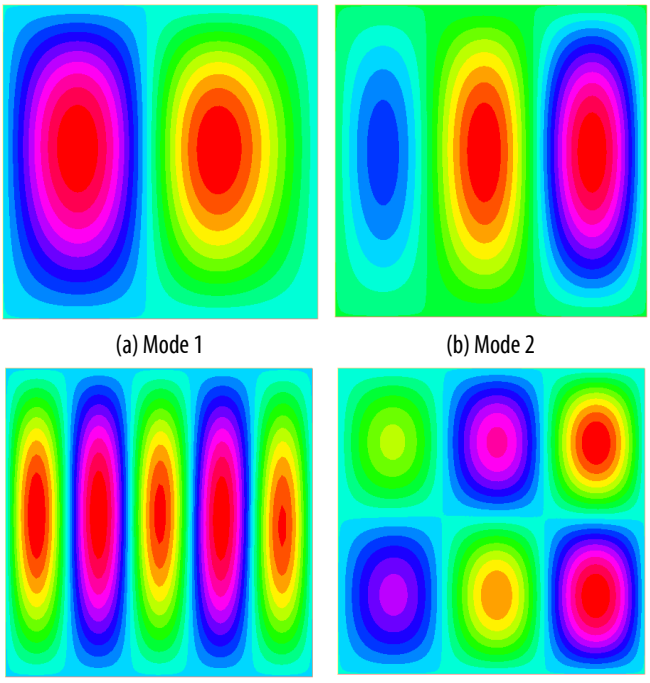

(a) Mode 1 (b) Mode 2

(c) Mode 3 (d) Mode 4

Figure 6. The first four buckling mode shapes of the FGM plate corresponding to the SSSS case, $\left[\hat{k}_w, \hat{k}_s\right] = [10^4, 100]$, $c_w = 0.5$

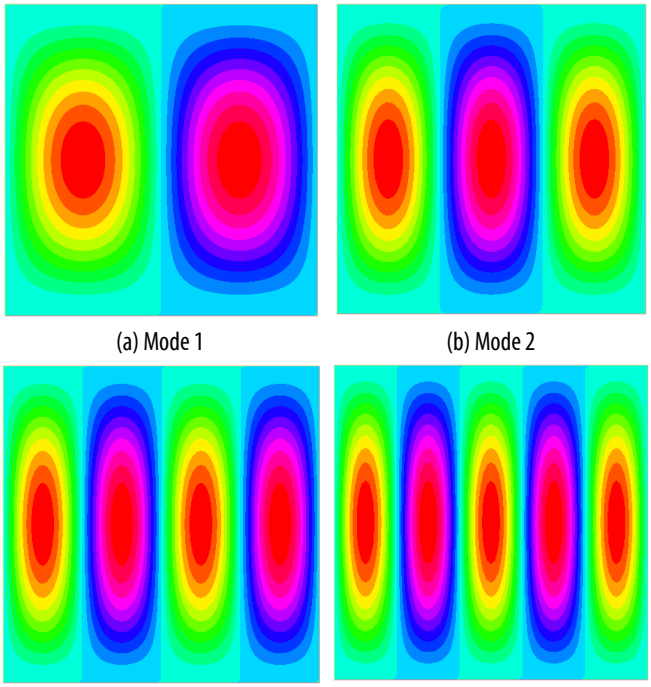

(a) Mode 1 (b) Mode 2

(c) Mode 3 (d) Mode 4

Figure 7. The first four buckling mode shapes of the FGM plate corresponding to the SCSC case, $\left[\hat{k}_w, \hat{k}_s\right] = [10^4, 100]$, $c_w = 0$

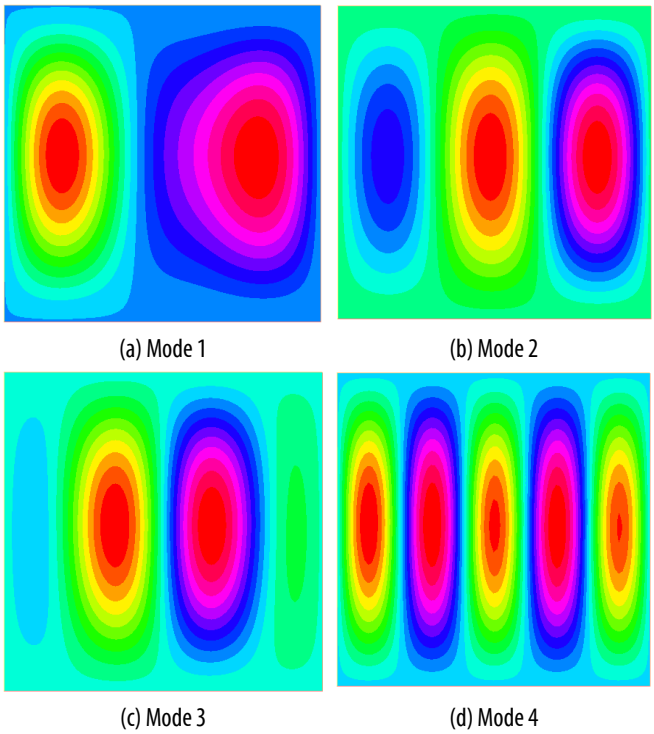

(a) Mode 1 (b) Mode 2

(c) Mode 3 (d) Mode 4

Figure 8. The first four buckling mode shapes of the FGM plate corresponding to the SCSC case, $\left[\hat{k}_w, \hat{k}_s\right] = [10^4, 100]$, $c_w = 0.5$

4. CONCLUSION

This article introduces a finite simulation approach for analyzing the static buckling behavior of functionally graded material (FGM) plates supported by an elastic base

with varying stiffness values. The plate's expressions and equilibrium equations are derived using Mindlin's first-order shear deformation theory. The assumption is made that the elastic basis has varying stiffness characteristics throughout the plane of the plate. In this work, a triangular plate element was used to solve the buckling equation of the plate. The paper also examined the impact of several parameters, such as materials, boundary conditions, and elastic basis, on the buckling behavior of this structure. This publication serves as a significant reference for the practical design and production of FGM plate structures.

REFERENCES

[1]. Dat PT., Luat DT., Thom DV., 2016. *Free vibration of functionally graded sandwich plates with stiffeners based on the third-order shear deformation theory*. Vietnam J Mech, 38/2, 103-122.

[2]. Thom DV., Doan DH., Tho NC., Duc N.D., 2022. *Thermal buckling analysis of cracked functionally graded plates*. Int J Struct Stab Dyn, 22/08, 2250089.

[3]. Vinh PV., Dung NT., N.C. Tho, Thom DV., Hoa LK,. 2021. *Modified single variable shear deformation plate theory for free vibration analysis of rectangular FGM plates*. Structures, 29, 1435-1444.

[4]. Quang DV., Doan TN., Luat DT., Thom, DV., 2021. *Static analysis and boundary effect of FG-CNTRC cylindrical shells with various boundary conditions using quasi-3D shear and normal deformations theory*. Structures, 44, 828-850.

[5]. Imam JM., Sundararajan N., Irwan K., 2022. *Application of discreste shear quadrilateral element for static bending, free vibration and buckling analysis of functionally graded material plate*. Comp Struct, 284, 51-87.

[6]. Thai HT., Kim SE., 2013. *Closed-form solution for bucking analysis of thick functionally graded plates on elastic foundation*. Int J Mech Sciences, 75, 34-44.

[7]. Yaghoobi H., Fereidoon A., 2014. *Mechanical and thermal buckling analysis of functionally graded plates resting on elastic foundations: An assessment of a simple refined nth-order shear deformation theory*. Comp Part B: Eng, 62, 54-64.

[8]. Sobhy M., Radwan AF., 2017. *A New Quasi 3D Nonlocal Plate Theory for Vibration and Buckling of FGM Nanoplates*. Int J Applied Mech, 9/1, 1-29.

THÔNG TIN TÁC GIẢ

Đào Mạnh Lân[1], Phan Quang Phúc[2], Phạm Văn Đông[3]

[1]Z131, Tổng cục Công nghiệp Quốc phòng

[2]Z183, Tổng cục Công nghiệp Quốc phòng

[3]Trường Đại học Công nghiệp Hà Nội